



## Low-temperature AMS and the quantification of subfabrics in deformed rocks



Josep M. Parés<sup>a,\*</sup>, Ben A. van der Pluijm<sup>b</sup>

<sup>a</sup> Geochronology Group, CENIEH, Paseo Sierra de Atapuerca 3, 09002 Burgos, Spain

<sup>b</sup> Department of Earth and Environmental Sciences, University of Michigan, Ann Arbor, MI 48109-1005, USA

### ARTICLE INFO

#### Article history:

Received 9 October 2013

Received in revised form 17 February 2014

Accepted 3 March 2014

Available online 11 March 2014

#### Keywords:

Anisotropy of Magnetic Susceptibility

Paramagnetism

Phyllosilicates

Low-temperature susceptibility

### ABSTRACT

We evaluate the application and significance of Low-Temperature Anisotropy of Magnetic Susceptibility (LT-AMS) measurements in deformed mudrocks. Originally conceived as a way to enhance paramagnetic relative to ferromagnetic susceptibility, LT-AMS studies offer significant potential in constraining the coexistence of subfabrics that are due to phyllosilicate grains with different preferred orientations. In this study we report a detailed procedure to obtain such directional susceptibilities, measuring samples in multiple orientations at liquid nitrogen temperatures in order to determine the LT-AMS. Due to unequal changes of magnetic susceptibility in micas at low-temperature, the enhancement of standard AMS at low-temperature better separates interacting fabrics in natural rocks, particularly depositional fabrics versus deformational fabrics. LT-AMS is a non-destructive technique that readily offers an ability to separate ferromagnetic and paramagnetic fabrics, and allows the characterization and quantification of multiple fabrics in natural rocks.

© 2014 Elsevier B.V. All rights reserved.

### 1. Introduction

Mudrocks typically contain more than 50% phyllosilicates by volume and about 30% quartz and feldspar and, while iron oxides (magnetite, hematite) and ferromagnesian minerals are common, the bulk magnetic susceptibility of mudrocks is often dominated by paramagnetism, reflecting the high phyllosilicate content. In low strain domains, where deformation is mostly accomplished by grain reorientation, the Anisotropy of Magnetic Susceptibility (AMS) as a proxy for preferred grain orientation offers an ideal fabric intensity gauge. The reasons that make the application of AMS a powerful approach in rock fabric analysis include: (1) Magnetic techniques are extremely sensitive to even very weak rock fabrics, (2) relatively large volumes of rock can be analyzed, which can be a limitation for other methods in inherently heterogeneous rocks, and (3) each measured sample integrates the properties of thousands of grains. Because virtually all rocks contain ferromagnetic grains, which typically have high magnetic susceptibility compared to paramagnetic grains, their contribution cannot be neglected. The distinction between the paramagnetic fabric and the ferromagnetic fabric is therefore a key issue that has attracted numerous studies. Indeed, the large body of literature on the linkage between AMS and deformation agrees that the distinction between paramagnetic and ferromagnetic fabrics lies at the heart of the use of AMS as a fabric intensity gauge. This paper offers an approach that better delineates fabric elements by applying AMS measurements at low temperature;

for practical reasons we use liquid nitrogen temperatures. We review results and limitations of the approach as successfully applied in several prior studies (Richter and van der Pluijm, 1994; Schultz-Krutsch and Heller, 1985; Lüneburg et al., 1999; Parés and van der Pluijm, 2002a, 2002b; Cifelli et al., 2009, among other), but also explore the potential of LT-AMS to determine magnetic ellipsoid shapes, where previous studies mainly emphasized the orientation of magnetic ellipsoids. A recent paper (Biedermann et al., 2014) explores the magnetic properties of micas and chlorite at low-temperature.

Through previous studies on mudrocks with variable degrees of preferred grain orientation, ranging from deep-sea sediments to mylonitic schists, we have gained a good understanding of preferred orientation of phyllosilicates and the evolution of rock fabrics using AMS techniques. There is a large literature that focuses on deformation fabrics, and the reader is referred to treatises such as Martín-Hernández et al. (2004) and Tarling and Hrouda (1993) and references therein, as well as seminal papers by Borradaile and Henry (1997) and Borradaile and Jackson (2010). Of particular interest are weakly deformed mudrocks, as studied in this paper, where mineral reorientation is sufficient to produce a weak, second mechanical anisotropy to the rocks, yet preserving the primary sedimentary fabric, resulting in two competing subfabrics.

#### 1.1. Magnetic fabric separation

The Low Field Magnetic Susceptibility of a rock (the ratio of magnetization to the applied field or  $K = M/H$ ) is given by the total contribution of its bulk mineralogy, including paramagnetic (e.g., phyllosilicates,

\* Corresponding author.

E-mail address: [josep.pares@cenieh.es](mailto:josep.pares@cenieh.es) (J.M. Parés).

iron-bearing feldspars), diamagnetic (e.g., quartz, calcite) and ferromagnetic (sensu lato; e.g., magnetite, goethite, hematite) grains. An intrinsic property of most rock-forming minerals is that Magnetic Susceptibility is anisotropic (Nye, 1957) and thus  $K_{ij} = M_i/H_j$ . The Anisotropy of Magnetic Susceptibility (AMS) in rocks depends mostly on the crystallographic preferred orientation of the individual components, compositional layering, distribution and size of microfractures, and the shape fabric of grains, which may interact in complex way (e.g., Hargraves et al., 1991). A corollary is that even rocks made by isotropic grains might have anisotropy due to unequal distribution or layering of their constituents. AMS defines a symmetric, second-rank tensor that has six independent matrix elements. When the coordinate system is referred to the eigenvectors, these trace an ellipsoid that is termed the magnitude ellipsoid (Nye, 1957) whose semi-axes are the three principal susceptibilities (maximum, intermediate and minimum susceptibility axes, or  $K_{\max}$ ,  $K_{\text{int}}$  and  $K_{\min}$  in the literature). AMS has been a popular tool in petrofabrics since Ising (1942) and Graham (1954) first proposed its application to geology, and it has successfully been used since then to investigate the spatial and geometrical configurations of the rock components for qualitative estimation of fabric development. Determination of preferred orientation of minerals is required in a variety of studies ranging from structural geology to permeability to velocity anisotropy (e.g., Vajdova et al., 1999). The AMS tensor tracks preferred orientation and consequently its applications have embraced a wide range of disciplines in Earth Sciences including tectonic fabrics (e.g., Borradaile, 1988; Borradaile and Henry, 1997; Housen et al., 1993; Parés and van der Pluijm, 2002a, 2002b), fault rocks (e.g., Solum and van der Pluijm, 2009), sedimentary depositional environments (e.g., Ellwood et al., 1979; Joseph et al., 1998; Kent and Lowrie, 1975; Parés et al., 2007; Park et al., 2000) and igneous rocks (e.g., Ellwood, 1982; Tauxe et al., 1998). The separation of ferromagnetic and paramagnetic susceptibilities, central to meaningful interpretation of magnetic fabrics, has progressively gained interest over the last 30 years, including mathematical and instrumental approaches. Next is a brief summary of the main methods.

By comparing AMS with the anisotropy of remanence it is theoretically possible to discriminate between the ferromagnetic and paramagnetic fabrics. Studies by McCabe et al. (1985), Stephenson et al. (1986), Housen and van der Pluijm (1991); Jackson (1991) and Lagroix and Borradaile (2000) used the anisotropy of anhysteretic remanent magnetization (AARM) to separate the ferromagnetic and paramagnetic tensors. The anisotropy of isothermal remanent magnetization (AIRM) has received less attention, but is an alternative approach to AARM (e.g., Borradaile and Dehls, 1993). Both AARM and AIRM involve magnetizing a sample repeatedly in different directions and measuring the intensity of the remanence that is acquired parallel to the applied field (Jackson, 1991; McCabe et al., 1985). We point out that, whereas AARM and AIRM are measures of remanent magnetism, AMS combines susceptibility and remanent contributions. Consequently, as emphasized by Borradaile et al. (1999), it is incorrect to simply subtract the two contributions as an approach to isolate one from the other.

A comprehensive description of the methods that aim to separate paramagnetic and ferromagnetic fabrics can be found in Martín-Hernández and Ferré (2007), so here we briefly summarize the existing instrumental methods.

#### 1.1.1. Cryogenic magnetometer (SQUID)

Although primarily designed for measuring remanence, Scriba and Heller (1978) and Schmidt et al. (1988) used a 100  $\mu\text{T}$  radial field and rotated the sample about each of three mutually perpendicular axes in steps of 45° and a total of 24 positions to determine the anisotropy tensor. Rochette and Fillion (1988) used a vertical-access SQUID magnetometer and trapped an applied field. By rotating the sample in a horizontal axis at a frequency of 0.01 Hz and analyzing the generated signal, they determined the susceptibility anisotropy of both ferromagnetic and paramagnetic fractions.

#### 1.1.2. Vibrating sample magnetometer (VSM)

The principle of VSM analysis is based on the flux change in the pick-up coil system produced by vibrating the sample (rather than by rotation, as in spinner magnetometers). Though primarily designed for the measurement of hysteresis properties, there have been attempts to use VSM's to obtain directional hysteresis curves for different positions of the specimen, hence enabling to the calculation of a High Field AMS (Ferre et al., 2004; Kelso et al., 2002; Thill et al., 2000). Borradaile and Werner (1994) successfully used an alternating gradient magnetometer to isolate the paramagnetic susceptibility of ferromagnetic inclusions in oriented phyllosilicate minerals. By changing the orientation of the sample in the holder, they repeated the measurements for different positions and extracted the magnetic anisotropy tensor.

#### 1.1.3. Torque magnetometer

This type of magnetometer is possibly the most popular instrument to measure high field magnetic susceptibility. The basic principle is the measurement of torque exerted on a sample by an applied magnetic field due to the anisotropy of the sample as it is rotated to different azimuths about an axis perpendicular to the field. The torque  $T$  is given by  $T = dE/d\theta$ , where  $E$  is the energy of magnetization of the sample and  $\theta$  is the direction of the applied field. It is thus possible to estimate the anisotropy present in the rock from a Fourier analysis of the torque curve. Applications can be found in Fletcher et al. (1969), Stacey and Banerjee (1974), Owens and Bamford (1976), Ellwood et al. (1979), Parma (1988) Bergmuller et al. (1994). Hrouda and Jelinek (1990) presented a mathematical method for separating the components by measuring as ample in two different fields above the saturation magnetization of the ferromagnetic contribution. More recently, Martín-Hernández and Hirt (2001) presented a mathematical method that utilizes measurements in several high fields toward separating the ferromagnetic and paramagnetic components of the magnetic fabric. By using a larger number of fields, instead of two as described by Lowrie (1989), a more accurate definition of the paramagnetic susceptibility tensor can be obtained.

The above three methods (cryogenic, vibrating, and torque magnetometers) have not been used on a systematic basis in magnetic fabric studies, although they have been gaining popularity (e.g., Martín-Hernández and Ferré, 2007; Martín-Hernández et al., 2006). Their main drawbacks are that they are time consuming, that they often require specific, that they are not standardized instrumentation, or that the necessary sample volume is too small to reliably extrapolate the results to the bulk rock unit.

High-temperature methods to separate magnetic fabrics rely on mineralogical and chemical reactions of mostly phyllosilicates when they are heated. These reactions are typically associated with the creation of newly-formed grains containing iron that translates into an increase of bulk magnetic susceptibility. Rather than isolate fabrics, heating methods enhance a pre-existing fabric at the expense of another. Temperatures above ca. 300 °C have been used to enhance the magnetic fabric of a variety of rocks (Lagroix and Borradaile, 2000; Perarnau and Tarling, 1985; Schultz-Krutisch and Heller, 1985; Urrutia-Fucugauchi and Tarling, 1983; Xu et al., 1991). Heating above such temperatures results in the formation of new minerals that can mimic the crystallographic structure of micas, the major carrier of AMS in the tested rocks. The heating method has been shown to be successful in some sandstones, siltstones and gneisses, whose magnetic fabrics have been determined after heating at different temperatures to enhance the susceptibility. However, there are two major drawbacks to high-temperature methods: 1) heating it is a non-reversible process and 2) changes in magnetic mineralogy need to be monitored, requiring additional analysis.

An alternative approach to heating the samples in order to enhance the bulk magnetic susceptibility is the use of low-temperature (LT) methods. The basis of low-temperature analysis is the dependence of the paramagnetic susceptibility on temperature. Whereas diamagnetic

susceptibility is independent of temperature, paramagnetic susceptibility follows the Curie–Weiss law. Also, ferromagnetic susceptibility is, to a first approximation, independent of temperature below the Curie point. Thus, the temperature dependence of susceptibility allows identification of the paramagnetic component of the magnetic fabric. For pure paramagnetic substances, the bulk magnetic susceptibility increases linearly with decreasing temperature, and at 77 K (a temperature achieved with liquid nitrogen) the measurements of directional susceptibility allow a definition of the paramagnetic anisotropy. An inherent limitation is the presence of superparamagnetic (SP) grains in the sample, whose susceptibility also is temperature dependent. However, SP contribution can be readily tested with dual frequency susceptibility determinations or by monitoring the change of remanence at low-temperature. Importantly, as opposed to heating procedures, low-temperature measurements do not carry associated mineral or other irreversible chemical changes. LT methods, based on “heating curves” from 77 K to room temperature, have been successfully applied to separate the paramagnetic and ferrimagnetic contributions in rocks (Ihmlé et al., 1989; Jover et al., 1989; Richter and van der Pluijm, 1994) but rarely to determine the anisotropy tensors, with the exception of Schultz-Krutisch and Heller (1985), Lunenburg et al. (1999), Parés and van der Pluijm (2002a), and Cifelli et al. (2009) and a few others.

## 2. LT-AMS: theoretical basis

Paramagnetic susceptibility in sheet silicates is mostly related to the presence of iron. If magnetic interactions are neglected, the magnetic susceptibility follows a Curie law (e.g., Morrish, 1965),  $X_p = C / (T - \theta)$ , where  $X_p$  is the mass susceptibility,  $C$  is the Curie constant,  $T$  is the absolute temperature and  $\theta$  is the paramagnetic Curie temperature. Plots of inverse susceptibility versus temperature give the paramagnetic Curie temperature,  $\theta$ , with the following characteristics. When negative, the material is antiferromagnetic; when positive, the material is ferromagnetic (see Dunlop and Ozdemir, 1997). As the magnetic ordering transition temperature is approached the paramagnetic susceptibility  $X_p$  increases considerably (Fig. 1).

Based on this intrinsic property, a practical method to measure the Low-Temperature (77 K) AMS was developed (Parés and van der Pluijm, 2002a). Since paramagnetic susceptibility increases significantly with low temperature, it allows high precision determination of the anisotropy of paramagnetic susceptibility from measurements at liquid nitrogen temperature. The procedure measures directional susceptibility in an oriented rock specimen while immersed in liquid nitrogen. Our

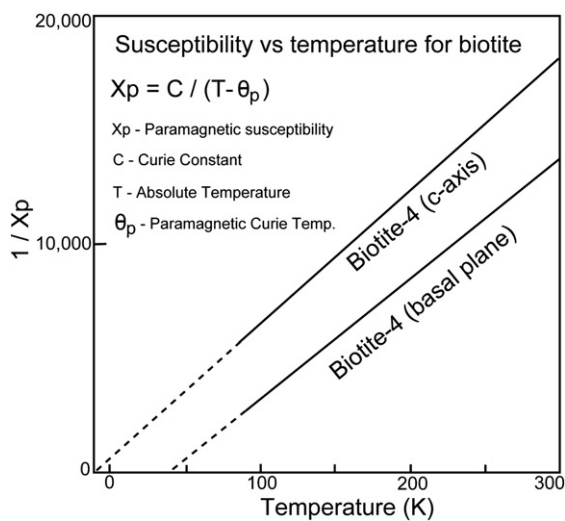


Fig. 1. Inverse relationship of susceptibility and temperature for biotite sample 4 (modified from Beausoleil et al., 1983). Measurements are done along the  $c'$  axis (top curve) and along the basal plane of the biotite sample.

method overcomes the problem of temperature heterogeneity in a rock sample, offering the opportunity to compare and combine low temperature susceptibility of multiple orientations.

## 3. Method

Previous attempts (Jover et al., 1989; Richter and van der Pluijm, 1994; Schmidt et al., 2007a; Schultz-Krutisch and Heller, 1985) showed that Low-Temperature susceptibility curves can be used for the separation of paramagnetic and ferrimagnetic bulk susceptibilities in a rock. However, Low-Temperature magnetic susceptibility has not been systematically applied to measure the magnetic fabric of rocks. Determination of “true” LT-AMS requires measurement of directional susceptibilities at a constant, low temperature; for practical reasons, liquid nitrogen temperature (77 K) is used. Accurate readings of the anisotropy of magnetic susceptibility require a uniform sample temperature during measurement. Measuring the sample at room temperature after cooling to 77 K introduces drift due to changing temperature of the specimen as it warms up. To overcome this problem, we designed a special, all-glass Dewar flask (double-walled, un-silvered) that is placed into a Sapphire Instruments 2B (SI2B) coil (Fig. 2). This arrangement permits measuring the magnetic susceptibility of a sample while it is immersed in liquid nitrogen and hence homogeneously cooled at 77 K. The SI2B coil unit is placed vertically, and the glass dewar containing liquid nitrogen rests inside the SI2B coil. A thin jacket of styrofoam is placed around the glass dewar to further protect the coil from excessive cooling. The holder is made of a combination of Mylar, plexiglass and Scotch tape and it fits tightly into the glass dewar (Fig. 2). After multiple tests, we determined that the LT-AMS tensor is fully determined from a six-orientation scheme, measuring every position twice ( $M = 6, N = 2$ ). This scheme takes the same time as  $M = 12$  and  $N = 1$ , but gives more precise principal susceptibility directions (Stupavsky, 1984). An additional advantage using the SI2B susceptibility meter is that it determines magnetic susceptibility by measuring the coil without the sample and then again with the sample. Thus, any diamagnetic contribution of the glass flask, liquid nitrogen and foam, is fully compensated. Lastly, the capacitance of the dewar containing liquid nitrogen does not cause spurious changes in coil frequency because liquid nitrogen has a dielectric constant of 1.4.

Our procedure consists of (1) immersing a sample holder with sample in a standard, 350 ml cylindrical, wide mouth liquid nitrogen dewar for about twenty minutes; (2) pouring liquid nitrogen into the empty flask seated in the SB2 coil, placed upright and letting the configuration stabilize; (3) immersing the sample holder into the flask, which is repeated for six orientations. The sample stays in the nitrogen-filled flask while the blank measurement is done. A standard program allows computing the main directional susceptibilities ( $K_{max}$ ,  $K_{int}$ ,  $K_{min}$ ) and related uncertainties from the measurements.

### 3.1. A LT-AMS case study: the Knobs Formation

In a previous study we examined AMS-strain linkages in pencil structures in the mudrocks from the Knobs Formation (Ordovician, Valley and Ridge Province, Appalachians; Parés and van der Pluijm, 2003). Because AMS commonly reflects the bedding–cleavage intersection in weak- to moderately-cleaved mudrocks, these well-studied samples provided an excellent opportunity to explore the type of information that is obtained by low-temperature susceptibility in deformed rocks. The prior AMS data revealed that the distribution of the magnetic ellipsoid axes tracks the incipient tectonic fabric of pencil-cleavage mudstones: maximum susceptibility axis typically parallels the pencils' long axes, while the minimum axis of susceptibility is normal to the primary sedimentary fabric (Fig. 3). Independent strain quantification from fringe (vein) structures (Reks and Gray, 1982) allows a correlation between magnetic fabric and tectonic strain (Parés and van der Pluijm, 2003). We determined an exponential relationship between the AMS

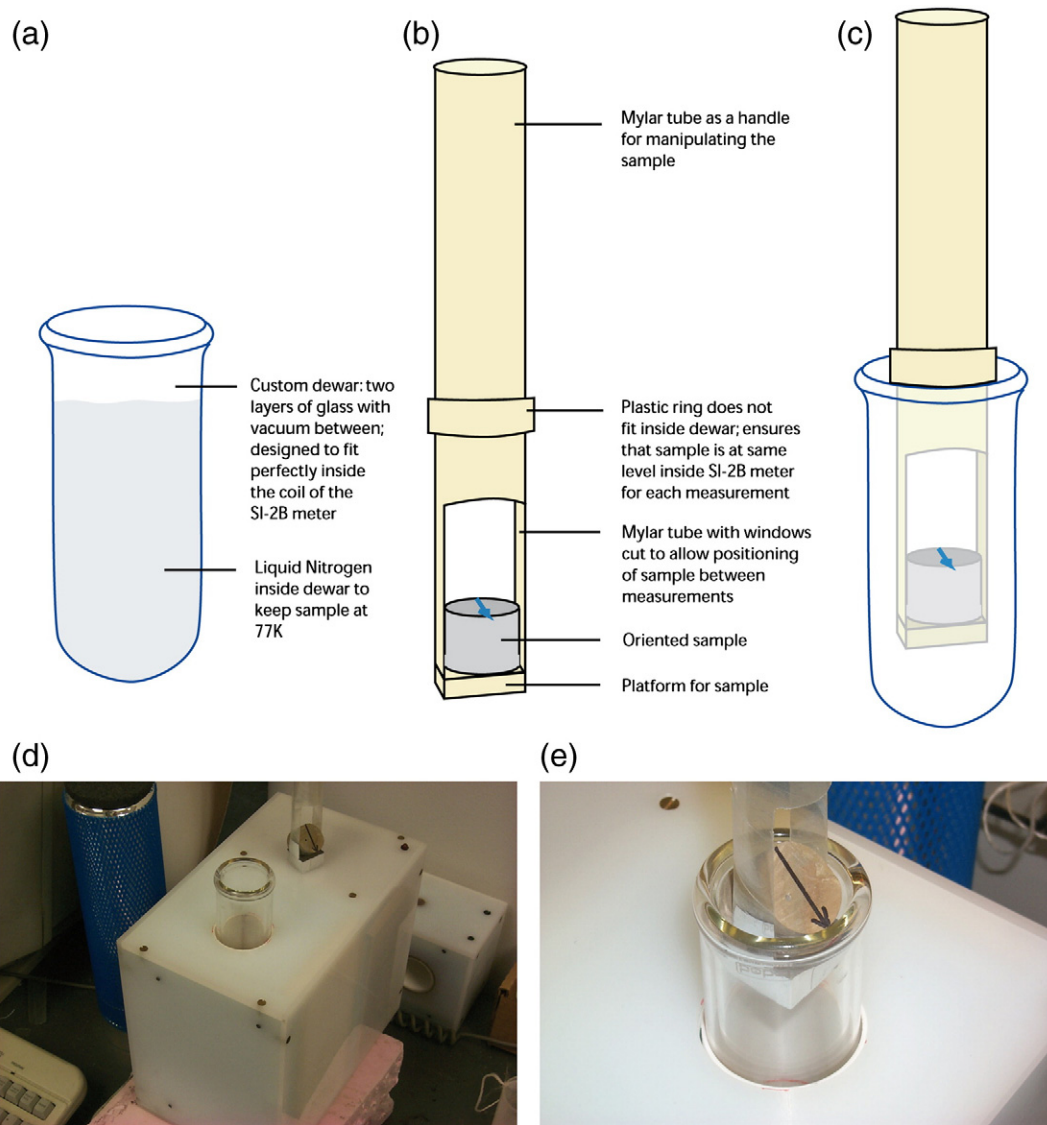


**Fig. 2.** Illustration of the setup for measurement of Low-Temperature AMS at liquid nitrogen temperature, requiring relatively inexpensive equipment and supplies. (a) Dewar where measurements are made and which is placed into the measuring coil; (b) Detail of the holder containing the sample to be measured; (c) Sample holder into the dewar; (d) top view of the SI2B coil including the dewar shown in (a); (e) detail of sample introduction.

shape parameter  $T$  and the strain for the interval of 10–25% shortening, and tectonic stain as high as 40%. The  $T$  parameter ( $T = [\ln F - \ln L] / [\ln L + \ln F]$ ) is used to describe the shape of the magnetic susceptibility

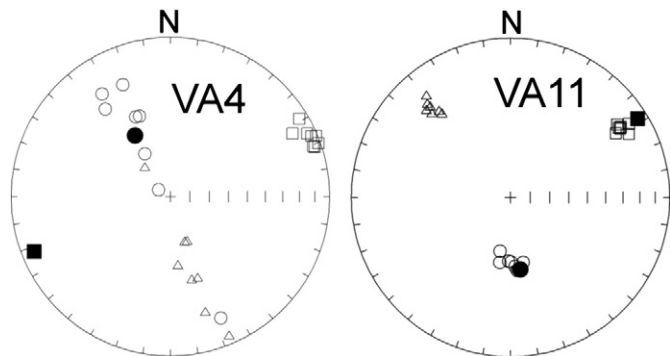


**Fig. 3.** Principal susceptibility axes (Squares –  $K_{max}$ , triangles –  $K_{int}$ , circles –  $K_{min}$ ) measured at room temperature for two sites of Knobs Fm. shales (modified from Parés and van der Pluijm, 2003). Dots show normal to bedding and filled squares show the pencil long axis orientation.

ellipsoid and better correlates with strain than the magnetic intensity parameter ( $P$  or  $P'$ ). Both  $T$  and  $P'$  values for measurements at low temperature were obtained, which are examined next.

A subset of the Knobs Fm. mudstones was selected for AMS measurement at both room and liquid nitrogen temperatures, following the method described above. For the bulk susceptibility, the average

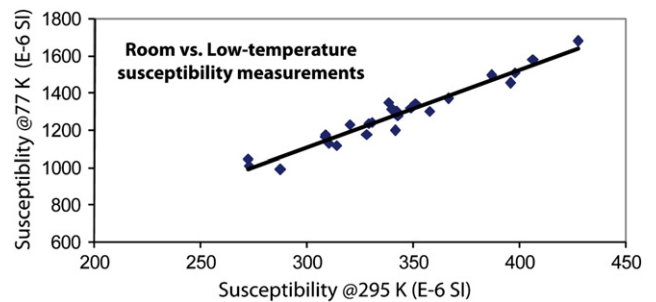


**Fig. 4.** Bulk susceptibility of Knobs Fm. samples measured at room temperature (X-axis) and at 77 K (Y-axis). Correlation shows a ratio of 3.7, which is consistent with a dominant paramagnetic contribution to the susceptibility.

ratio ( $K_{77}/K_{295}$ ) is 3.7 (Fig. 4), revealing almost ideal paramagnetic behavior (Parés and van der Pluijm, 2002a, 2002b; Richter and van der Pluijm, 1994). Rather than focusing on the AMS axis distributions as the previous studies do, we examine changes in the magnetic ellipsoid shape and ellipticity. We observe significant, systematic changes when magnetic anisotropy is measured at low temperature. On a Flinn-type diagram, the increase of both lineation and foliation of the LT-AMS is apparent, and reveals disproportional change in the axial ratios of the principal susceptibility axes (Fig. 5). This was observed before in single mica grains, in which the increase of susceptibility at low temperature is unequal along and across the crystallographic *c* axis (Beausoleil et al., 1983). As susceptibility in our samples is dominated by paramagnetic behavior, the LT measurement results reflect this intrinsic property of phyllosilicates. At low temperature, the interactions within a crystallographic plane in sheet iron-silicate grains are far greater than the interactions between planes (e.g., Beausoleil et al., 1983). Such weaker interplane coupling at low temperatures translates to an increase of the magnetic anisotropy ( $K_{max}/K_{min}$ ) (Fig. 5). The susceptibility of biotite is similarly more anisotropic at low temperatures that was previously noted (e.g. Ballet and Coey, 1982), and similar observations have been made in other iron-bearing phyllosilicates (Ballet and Coey, 1982; Ballet et al., 1985). The explanation of these results is that, at low temperatures, when the susceptibility is sufficiently large, spontaneous ferromagnetic order appears within the plane of the sheets and not across them. As a result, the anisotropy degree ( $K_{max}/K_{min}$ ) increases when measured at 77 K.

To fully evaluate the magnetic fabric changes at low temperature, we separately plot both the anisotropy degree (*P*) and the shape parameter (*T*) of the fabric. The resulting changes of these parameters with temperature are illustrated in Fig. 6a, where the best fitting lines for *P* and *T* have been added. The regression line for *T* data has a near-unit slope of 0.92, whereas the slope for *P* is 1.95, revealing that *T*, on average, is essentially independent of the temperature at which the sample is measured. We also see that *T* tends to shift toward or into the oblate field at Low-Temperature when the original fabric is prolate ( $T < 0$ ) (Fig. 6b). In other words, the largest changes in *T* occur for the most prolate ellipsoids. In contrast, variation in *T* is minimal for samples in the oblate field. This contrasting behavior occurs because, at liquid nitrogen temperature, there is a change in the axial ratio of the principal susceptibility axes of phyllosilicates, as discussed earlier, and, consequently, the degree of anisotropy changes. In contrast to changes in shape, the anisotropy degree is greatly enhanced by low-temperature

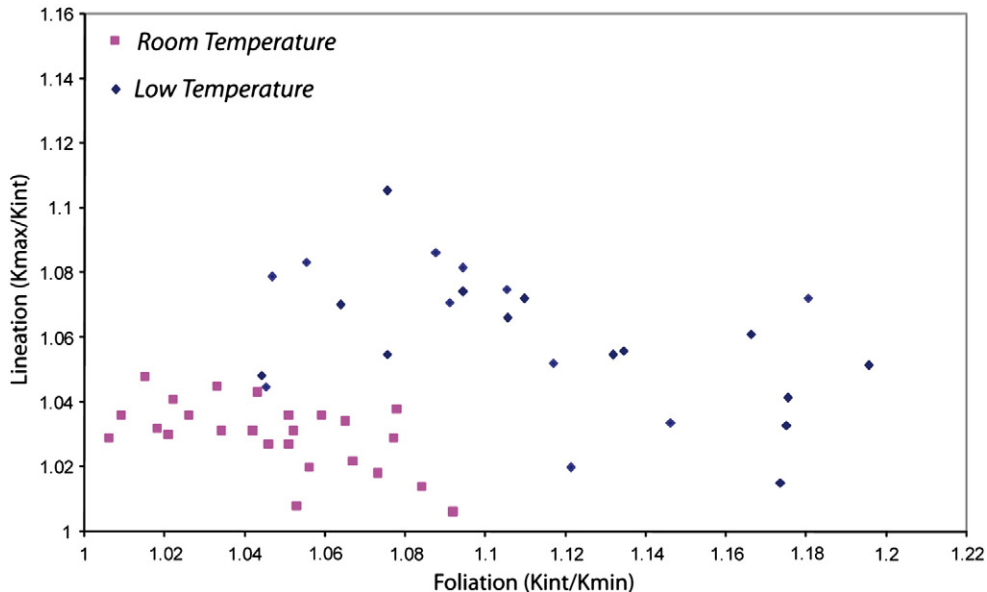


Fig. 5. Flinn-type diagram with susceptibility values for Knobs Fm. samples. Squares and diamonds are the results at room temperature and at 77 K, respectively.

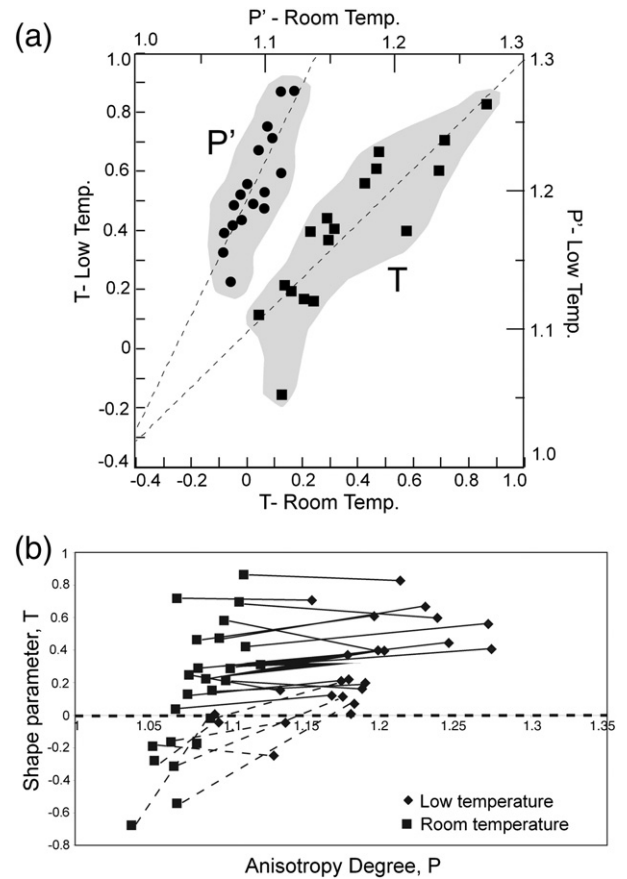


Fig. 6. (a) Values of the degree of anisotropy (*P'*) and the ellipsoid shape parameter (*T*) measured at room temperature and at liquid nitrogen temperature. Dashed lines show the best fit for both sets of data. (b) Measurements for individual samples (room temperature, low temperature) are connected with dashed lines. See text for discussion.

measurements, resulting in change by a multiplication factor of almost ~2 (see also Schmidt et al., 2007b). In summary, for oblate ellipsoids, changes in *P* tend to be less pronounced, and *T* (ellipsoid shape) remains mostly constant. When *T* has negative values, representing prolate shapes, changes in *P* are smaller while *T* tends to move toward

the oblate field. We hypothesize that this behavior can be used to decipher the origin of the magnetic fabric, as discussed below.

### 3.2. Interpretation

The changes of magnetic parameters when measurements are made at 77 K represent the origin and properties of magnetic fabrics, reflecting the uneven growth of susceptibility in mica grains at low temperature. Samples the Knobs Fm. shales preserve both oblate and prolate types of AMS fabrics (see details in Parés and van der Pluijm, 2003). Field end members from well-developed cleavage to no visible cleavage fall in the oblate field, whereas samples with moderate cleavage fall in the prolate field. This progression in shales allows us to evaluate the meaning of the LT AMS measurements. As described in the previous section, the oblate ellipsoids with lower ellipticity values experience larger changes in the anisotropy degree at low temperature (Fig. 6b). On the other hand, the value of T remains mostly constant for these samples. To understand these patterns at low-temperature we need to look at the corresponding fabrics at room temperature.

The magnetic anisotropy in the Knobs Fm. shales reflects the competing effects of two foliations that intersect at high angles, producing the characteristic pencil structures in the field (Reks and Gray, 1982). A subhorizontal fabric is parallel to bedding, and a second, steeply-dipping fabric, which is less apparent at outcrop level, is parallel to regional cleavage. The relative amount of phyllosilicate grains contributing to one or the other foliation, and the angle between these two foliations, ultimately determines the degree of anisotropy. Measurements at 77K reveal that, when one fabric dominates (high T positive values), changes of P parameter are pronounced. In contrast, when two subsets of phyllosilicate fabrics compete (low or negative T values), the changes in anisotropy values are less at low temperature. Thus, we can use this behavior to examine fabrics of unknown origin. Fig. 7 is a conceptual model where we compare the change of the anisotropy degree P at room and low temperatures, from which we infer the relationship between competing fabrics. Since the angle between fabrics is typically resolved in the field (e.g., angle between bedding and cleavage or flattening plane), this theoretical relationship provides a first estimate of the relative contribution of each competing fabrics in the rocks. Two subfabrics typically compete in shales, a depositional fabric and a shortening (flattening) fabric, defining the total anisotropy, which, by using the proposed ratio here, the relative contribution of these two subfabrics can be estimated. Calibration of the function depicted in Fig. 7 requires determining LT-AMS in rocks with known subfabrics.

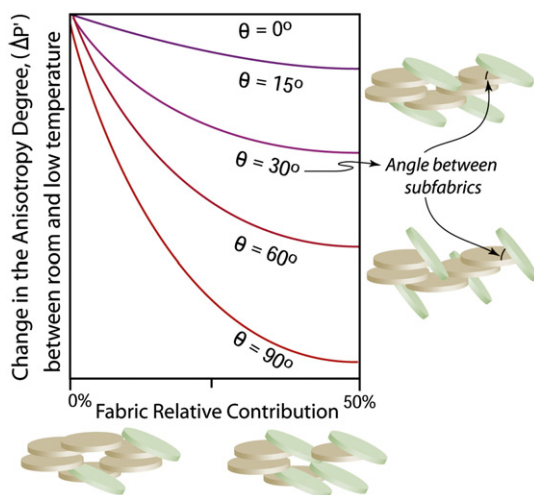


Fig. 7. Conceptual model of change of anisotropy degree (vertical axis) measured at room and low-temperature. Change is shown as  $(\Delta P = P_{77K} - P_{293K}) / P_{293K}$ . Horizontal axis represents two contributing fabrics that form an angle  $\theta$  between them. Different lines show the changes in the angle  $\theta$ , as shown on the right side of the axis.

The origin of prolate ellipsoids in shales and slates that contain two subfabrics, as illustrated in this paper by samples from the Knobs Fm., is the intersection lineation of these phyllosilicate fabrics (or zone axis), as previously discussed by several authors (Borradaile, 1987; Borradaile and Henry, 1997; Housen et al., 1993; Parés and van der Pluijm, 2003; Weil and Yonkee, 2009). The orientation of phyllosilicate grains aligned about the tectonic extension direction, or what Henry (1997) called the magnetic zone axis is then expressed as a magnetic lineation and thus ellipsoids are typically prolate. At low-temperature we see that such prolate ellipsoids, due to uneven growth of susceptibility within and across phyllosilicate grains, tend to move toward the oblate field. Phyllosilicates, such as micas, have almost ideal oblate magnetic anisotropy ( $T = 0.96 \pm 0.02$ , Martin-Hernández, and Hirt, 2003), so, when their  $c'$  axes are slightly rotated relative to each other, the zone distribution produces a marked magnetic lineation. Due to the changes in the axial ratio of susceptibilities at low temperature, these prolate ellipsoids move toward the oblate field (Fig. 6). The change of T parameter values at low temperature has valuable implications for the interpretation of magnetic lineations in deformed rocks. In samples of the Knobs Fm., the magnetic lineation is due to the intersection axis that aligned with the tectonic extension (i.e., long axes of the pencil structures or the bedding–cleavage intersection) (Pares and van der Pluijm, 2003). In depositional environments, however, the magnetic lineation is often due to the preferred orientation of  $K_{max}$  axes of individual grains (e.g., Parés et al., 2007). In such cases, the magnetic lineation is not the zone axis around which the basal plane of platelet-shaped grains rotate, but instead the dominant orientation of the grains' long axes. Because the measured magnetic lineation does not correspond to the zone axis, the enhancement of susceptibility at low temperature will display a different effect. In our example with prolate ellipsoids, they trend toward the oblate field when measured at 77 K. However, we anticipate that ellipsoids with a magnetic lineation due to clustering of  $K_{max}$  axes, will likely stay in the prolate field, and not move toward the oblate field. This is because, at low temperature, the susceptibility axes along the basal plane of micas increase proportionally more than along the crystallographic  $c$  axis, and hence the bulk effect will retain the prolate magnetic fabric even at low temperature. This behavior, if corroborated, would provide a novel means to distinguish between magnetic lineations due to the zone axis of non-parallel subfabrics from that produced by grain long axes preferred orientation. Further experiments in a range of samples that preserve varying degrees and types of deformations will allow us to determine in more details the changes of magnetic ellipsoids when measured at low temperature.

### 4. Conclusion

There are multiple advantages of measuring susceptibility anisotropy at liquid nitrogen temperature (here called LT-AMS). Because it obeys the Curie–Weiss Law, the bulk susceptibility of mica increases by a factor about 3.7, making the signal much stronger than background noise of the instrument and provides better definition of the magnetic fabric as it increases magnetic anisotropy (P parameter). In sedimentary rocks that typically contain composite magnetic fabrics (i.e., a depositional fabric and layer parallel shortening or shear fabrics), the change in anisotropy degree from room to low-temperature measurements can be used to estimate the relative contribution of the subfabrics. We also offer a conceptual model that holds promise for better characterization of composite AMS fabric elements in naturally-deformed rocks. In the case of rocks with a magnetic lineation, a common situation in weakly deformed shales, low temperature measurement produces two effects. When prolate ellipsoids are due to a zone axis of mica basal planes, the ellipsoids will tend to become more oblate when measured at low temperature. With originally prolate ellipsoids due to the preferred orientation of grain long axes, the results tend to remain in the prolate field. This contrast provides a relatively easy approach to

better constrain the origin of (composite) magnetic fabrics in weakly to moderately-deformed sedimentary rocks.

## Acknowledgments

Our research on magnetic susceptibility has been funded by grants from the US National Science Foundation and the International Ocean Drilling Program. We thank Laura Holladay for AMS analysis at the University of Michigan that is included in this paper. We also like to thank Graham Borradaile (and associates) for many insightful contributions to the study of magnetic anisotropy and deformation, several of which are referenced in this paper. We also thank two anonymous reviewers for their helpful comments that have improved the final version of this paper.

## References

- Ballet, O., Coey, J.M.D., 1982. Magnetic properties of sheet silicates; 2:1 layer minerals. *Phys. Chem. Miner.* 8, 218–229.
- Ballet, O., Coey, J.M.D., Burke, K.J., 1985. Magnetic properties of sheet silicates; 2:1:1 layer minerals. *Phys. Chem. Miner.* 12, 370–378.
- Beausoleil, N., Lavalley, P., Yelon, A., Ballet, O., Coey, J.M.D., 1983. Magnetic properties of micas. *J. Appl. Phys.* 54, 906–915.
- Bergmuller, F., Barlocher, C., Geyer, B., Heller, F., Zweifel, P., 1994. A torque magnetometer for measurement of the highfield anisotropy of rocks and crystals. *Meas. Sci. Technol.* 5, 1466–1470.
- Biedermann, A.R., Koch, C.B., Lorenz, W.E.A., Hirt, A.M., 2014. Low-temperature magnetic anisotropy in micas and chlorite. *Tectonophysics* 629, 63–74.
- Borradaile, G.J., 1987. Anisotropy of magnetic susceptibility: rock composition versus strain. *Tectonophysics* 138, 327–329.
- Borradaile, G.J., 1988. Magnetic susceptibility, petrofabrics and strain. *Tectonophysics* 156, 1–20.
- Borradaile, G., Dehls, J.F., 1993. Regional kinematic inferred from magnetic subfabrics in Archean rocks of Northern Ontario. *Can. J. Struct. Geol.* 15, 887–894.
- Borradaile, G.J., Henry, B., 1997. Tectonic applications of magnetic susceptibility and its anisotropy. *Earth Sci. Rev.* 42, 49–93.
- Borradaile, G.J., Jackson, M., 2010. Structural geology, petrofabrics and magnetic fabrics (AMS, AARM, AIRM). *J. Struct. Geol.* 32, 1519–1551.
- Borradaile, G.J., Fralick, P.W., Lagroix, F., 1999. Acquisition of anhysteretic remanence and tensor subtraction from AMS isolates true palaeocurrent grain alignments. In: Tarling, D.H., Turner, P. (Eds.), *Palaeomagnetism and Diagenesis in Sediments*. Geol. Soc. Lond. Sp. Publ., 151, pp. 139–145.
- Borradaile, G.J., Werner, T., 1994. Magnetic anisotropy of some phyllosilicates. *Tectonophysics* 235, 223–248.
- Cifelli, F., Mattei, M., Chadima, M., Lenser, S., Hirt, A.M., 2009. The magnetic fabric in “undeformed clays”: AMS and neutron texture analyses from the Rif Chain (Morocco). *Tectonophysics* 466, 79–88.
- Dunlop, D., Ozdemir, 1997. *Fundamentals and frontiers*, Cambridge University Press, Rock Magnetism.
- Ellwood, B.B., 1982. Estimates of flow direction for calc-alkaline welded tuffs and paleomagnetic data reliability from anisotropy of magnetic susceptibility measurements; central San Juan Mountains, Southwest Colorado. *Earth Planet. Sci. Lett.* 59, 303–314.
- Ellwood, B.B., Ledbetter, M.T., Johnson, D.A., 1979. Sedimentary fabric tool to delineate a high velocity zone within a deep Western Indian Ocean bottom current. *Marine Geol.* 33, 51–55.
- Ferre, E.C., Martín-Hernández, F., Teyssier, C., Jackson, M., 2004. Paramagnetic and ferromagnetic anisotropy of magnetic susceptibility in migmatites: measurements in high and low fields and kinematic implications. *Geophys. J. Int.* 157, 1119–1129.
- Fletcher, E.J., de Sa, A., O'Reilly, W., Banerjee, S.K., 1969. A digital vacuum torque magnetometer for the temperature range 300–1000°K. *J. Phys. E: Sci. Instrum.* 2:311.
- Graham, J.W., 1954. Magnetic susceptibility anisotropy, an unexploited petrofabric element. *Geol. Soc. Am. Bull.* 65, 1257–1258.
- Hargraves, R.B., Johnson, D., Chan, C.Y., 1991. Distribution anisotropy: the cause of AMS in igneous rocks? *Geophys. Res. Lett.* 18, 2193–2196.
- Henry, B., 1997. The magnetic zone axis: a new element of magnetic fabric for the interpretation of the magnetic lineation. *Tectonophysics* 271, 325–331.
- Housen, B.A., van der Pluijm, B.A., 1991. Slaty cleavage development and magnetic anisotropy fabrics (AMS and ARMA). *J. Geophys. Res.* 96, 9937–9946.
- Housen, B.A., Richter, C., van der Pluijm, B.A., 1993. Composite magnetic anisotropy fabrics: experiments, numerical models, and implications for the quantification of rock fabrics. *Tectonophysics* 220, 1–12.
- Hrouda, F., Jelinek, V., 1990. Resolution of ferrimagnetic and paramagnetic anisotropies in rocks, using combined low field and high field measurements. *Geophys. J. Int.* 103, 75–84.
- Ihmlé, P., Hirt, A.M., Lowrie, W., Dietrich, D., 1989. Inverse magnetic fabric in deformed limestones of the Morcles Nappe, Switzerland. *Geophys. Res. Lett.* 16, 1383–1386.
- Ising, G., 1942. On the magnetic properties of varved clay: *ark. Mater. Astron. Fysiol.* 29a, 1–37.
- Jackson, M., 1991. Anisotropy of magnetic remanence: a brief review of mineralogical sources, physical origins, and geological applications, and comparison with susceptibility anisotropy. *Pure Appl. Geophys.* 136, 1–28.
- Joseph, L.H., Rea, D.K., van der Pluijm, B.A., 1998. Use of grain size and magnetic fabric analyses to distinguish among depositional environments. *Paleoceanography* 13, 491–501.
- Jover, O., et al., 1989. Magnetic mineralogy of some granites from the French Massif Central: origin of their low-field susceptibility. *Phys. Earth Planet. Inter.* 55, 79–92.
- Kelso, P., Tikoff, B., Jackson, M., Sun, W., 2002. A new method for the separation of paramagnetic and ferromagnetic susceptibility anisotropy using low field and high field methods. *Geophys. J. Int.* 151, 345–359.
- Kent, D.V., Lowrie, W., 1975. On the magnetic susceptibility anisotropy of deep-sea sediment. *Earth Planet. Sci. Lett.* 28, 1–12.
- Lagroix, F., Borradaile, G.J., 2000. Magnetic fabric interpretation complicated by inclusions in mafic silicates. *Tectonophysics* 325, 207–225.
- Lowrie, W., 1989. Magnetic analysis of rock fabric. In: James, D.E. (Ed.), *The Encyclopedia of Solid Earth Geophysics*: New York (Van Nostrand Reinhold), pp. 698–706.
- Luneburg, C.M., Lampert, S.A., Lebit, H.K., Hirt, A.M., Casey, M., Lowrie, W., 1999. Magnetic anisotropy, rock fabrics and finite strain in deformed sediments of SW Sardinia (Italy). *Tectonophysics* 307, 51–74.
- Martín-Hernández, F., Hirt, A.M., 2001. Separation of ferrimagnetic and paramagnetic anisotropies using a high-field torsion magnetometer. *Tectonophysics* 337, 209–221.
- Martín-Hernández, F., Hirt, A., 2003. Paramagnetic anisotropy of magnetic susceptibility in biotite, muscovite and chlorite single crystals. *Tectonophysics* 367, 13–28.
- Martín-Hernández, F., Ferré, E.C., 2007. Separation of paramagnetic and ferrimagnetic anisotropies. *J. Geophys. Res.* 112 (B3). <http://dx.doi.org/10.1029/2006JB004340>.
- Martín-Hernández, F., Luneburg, C.M., Aubourg, C., Jackson, M. (Eds.), 2004. *Magnetic Fabric: Methods and Applications*. Geological Society, London, Special publications, 238.
- Martín-Hernández, F., Bominaar-Silkens, I., Dekkers, M.J., Maan, J.K., 2006. High-field cantilever torque magnetometry as a tool for single crystal magnetocrystalline anisotropy determinations. *Tectonophysics* 418, 21–30.
- McCabe, C., Jackson, M., Ellwood, B., 1985. Magnetic anisotropy in the Trenton limestone: results of a new technique, anisotropy of anhysteretic susceptibility. *Geoph. Res. Lett.* 12, 333–336.
- Morrish, A.H., 1965. *The physical principles of magnetism*. Wiley, New York, pp 680.
- Nye, J.F., 1957. *Physical Properties of Crystals*. Oxford Univ. Press, London (322 pp).
- Owens, W.H., Bamford, D., 1976. Magnetic, seismic and other anisotropic properties of rock fabrics. *Phil. Trans. R. Soc. Lond. A* 283, 55–68.
- Parés, J.M., van der Pluijm, 2002a. Phyllosilicate fabric characterization by Low-Temperature Anisotropy of Magnetic Susceptibility (LT-AMS). *Geophys. Res. Lett.* <http://dx.doi.org/10.1029/2002GL015459>.
- Parés, J.M., van der Pluijm, B., 2002b. Evaluating magnetic lineation (AMS) in deformed rocks. *Tectonophysics* 350, 283–298.
- Parés, J.M., van der Pluijm, B.A., 2003. Magnetic fabrics in low-strain mudrocks: AMS of pencil structures in the Knobs Formation, Valley and Ridge Province, US Appalachians. *J. Struct. Geol.* 25, 1349–1358.
- Parés, J.M., Hassold, N.J.C., Rea, D.K., van der Pluijm, B.A., 2007. Paleocurrent directions from paleomagnetic reorientation of magnetic fabrics in deep-sea sediments at the Antarctic Peninsula Pacific margin (OPD Sites 1095, 1101). *Mar. Geol.* 242, 261–269.
- Park, C.K., Doh, S.J., Suk, D.W., Kim, K.H., 2000. Sedimentary fabric on deep-sea sediments from KODOS area in the eastern Pacific. *Mar. Geol.* 171, 115–126.
- Parma, J., 1988. An automated torque meter for rapid measurement of high-field magnetic anisotropy of rocks. *Phys. Earth Planet. Inter.* 51, 387–389.
- Perarnau, A., Tarling, D.H., 1985. Thermal enhancement of magnetic fabric in Cretaceous sandstone. *J. Geol. Soc. Lond.* 142, 1029–1034.
- Reks, I.J., Gray, D.R., 1982. Pencil structure and strain in weakly deformed mudstone and siltstone. *J. Struct. Geol.* 4, 161–176.
- Richter, C., van der Pluijm, B.A., 1994. Separation of paramagnetic and ferrimagnetic susceptibilities using low-temperature magnetic susceptibilities and comparison with high field methods. *Phys. Earth Planet. Inter.* 82, 113–123.
- Rochette, P., Fillion, G., 1988. Identification of multicomponent anisotropies in rocks using various field and temperature values in a cryogenic magnetometer. *Phys. Earth Planet. Inter.* 51, 379–386.
- Schmidt, V.A., Ellwood, B., Nagata, T., Noltimier, H.C., 1988. The measurement of anisotropy of magnetic susceptibility using a cryogenic (SQUID) magnetometer and a comparison with results obtained from a torsion-fiber magnetometer. *Phys. Earth Planet. Inter.* 51, 365.
- Schmidt, V., Hirt, A.M., Rosselli, P., Martín-Hernández, F., 2007a. Separation of diamagnetic and paramagnetic anisotropy by high-field, low-temperature torque measurements. *Geophys. J. Int.* 168, 40–47.
- Schmidt, V., Hirt, A.M., Hametner, K., Günther, D., 2007b. Magnetic anisotropy of carbonate minerals at room temperature and 77 K. *Am. Mineral.* 92, 1673–1684.
- Schultz-Krutsch, T., Heller, F., 1985. Measurement of magnetic susceptibility anisotropy in Brunsandstein deposits from southern Germany. *J. Geophys.* 56, 51–58.
- Scriba, H., Heller, F., 1978. Measurements of anisotropy of magnetic susceptibility using inductive magnetometers. *J. Geophys.* 44, 341–352.
- Solum, J.G., van der Pluijm, B.A., 2009. Quantification of fabrics in clay gouge from the Carboneras Fault, Spain and implications for fault behavior. *Tectonophysics* 475, 554–562.
- Stacey, F.D., Banerjee, S.K., 1974. *The Physical Principles of Rock Magnetism*. Elsevier, Amsterdam, pp. 195.
- Stephenson, A., Sadikun, S., Potter, D.K., 1986. A theoretical and experimental comparison of the anisotropies of magnetic susceptibility and remanence in rocks and minerals. *Geophys. J. R. Astron. Soc.* 84, 185–200.

- Stupavsky, M., 1984. Operating manual for the SI-2 Magnetic susceptibility Instrument. Sapphire Instruments, PO Box 385, Ruthven, Ont., NOP 2G0, Canada.
- Tarling, D.H., Hrouda, F., 1993. *The Magnetic Anisotropy of Rocks*. Chapman and Hall, London (217 pp.).
- Tauxe, L., Gee, J.S., Staudigel, H., 1998. Flow directions in dikes from anisotropy of magnetic susceptibility data: the bootstrap way. *J. Geophys. Res.* (ISSN: 0148-0227) 103. <http://dx.doi.org/10.1029/98JB01077>.
- Thill, J.W., Ferré, E.C., Rainey, E.S.G., Teyssier, C., 2000. Separation of AMS into ferromagnetic and paramagnetic components in magnetites: a possible shear-sense indicator? *EOS Trans. Am. Geophys. Union* 81 (48), F367.
- Urrutia-Fucugauchi, J., Tarling, D.H., 1983. Palaeomagnetic properties of Eocambrian sediments in northwestern Scotland: implications for world-wide glaciation in the Late Precambrian. *Palaeogeogr. Palaeoclimatol. Palaeoecol.* 41, 325–344. [http://dx.doi.org/10.1016/0031-0182\(83\)90093-7](http://dx.doi.org/10.1016/0031-0182(83)90093-7).
- Vajdova, V., Prikryl, R., Pros, Z., Klíma, K., 1999. The effect of rock fabric on P-wave velocity distribution in amphibolites. *Phys. Earth planet. Inter.* 114, 39–47.
- Weil, A.B., Yonkee, A., 2009. Anisotropy of magnetic susceptibility in weakly deformed red beds from the Wyoming salient, Sevier thrust belt: relations to layer-parallel shortening and orogenic curvature. *Lithosphere* 1, 235–256.
- Xu, T.C., Ye, S.J., Yang, F., 1991. A preliminary study of thermally enhanced magnetic fabric in the Tertiary sediments from the Qidam Basin, NW China. *Stud. Geophys. Geol.* 35, 295–301.